CHAPTER 4.

Recent Drought Conditions in the Conterminous United States

Frank H. Koch
William D. Smith
John W. Coulston

INTRODUCTION

Droughts are common in virtually all U.S. forests, but their frequency and intensity vary widely both between and within forest ecosystems (Hanson and Weltzin 2000). Forests in the Western United States generally exhibit a pattern of annual seasonal droughts. Forests in the Eastern United States tend to exhibit one of two prevailing patterns: random occasional droughts, typical of the Appalachian Mountains and of the Northeast, or frequent late-summer droughts, typical of the Southeastern Coastal Plain and the eastern edge of the Great Plains (Hanson and Weltzin 2000). For plants, a reduction in basic growth processes (i.e., cell division and enlargement) is the most immediate response to drought; photosynthesis, which is less sensitive than these basic processes, decreases slowly at low levels of drought stress, but begins to decrease more sharply when the stress becomes moderate to severe (Kareiva and others 1993, Mattson and Haack 1987). Drought makes some forests more susceptible to infestations of tree-damaging insects and diseases (Clinton and others 1993, Mattson and Haack 1987). Furthermore, drought may increase wildland fire risk by impeding decomposition of organic matter and reducing the moisture content of downed woody materials and other potential fire fuels (Clark 1989, Keetch and Byram 1968, Schoennagel and others 2004).

Notably, forests appear to be relatively resistant to short-term drought conditions (Archaux and Wolters 2006), although individual tree species differ in their responses (Hinckley and others 1979, McDowell and others 2008). The duration of a drought event is arguably more significant than its intensity (Archaux and Wolters 2006); for example, multiple consecutive years of drought (2 to 5 years) are more likely to result in high tree mortality than a single dry year (Guarín and Taylor 2005, Millar and others 2007). This suggests that a comprehensive characterization of drought impact in forested areas should include analysis of moisture conditions in the United States over relatively long, i.e., multi-year, time windows.

In the FHM 2010 national report, we outlined a new methodology for mapping drought conditions across the conterminous United States (Koch and others 2013). As in previous work related to this topic (Koch and others 2012a, 2012b), a primary objective of this new methodology was to provide forest managers and researchers with drought-related spatial data sets that are finer-scale than products available from such sources as the National Climatic Data Center (2007) or the U.S. Drought Monitor program (Svoboda and others 2002). The primary inputs are gridded climate data, i.e., monthly raster maps of precipitation and temperature over a 100-year period, created with the Parameter-elevation Regression on Independent Slopes (PRISM) climate mapping system (Daly and others 2002). A pivotal aspect of our new methodology is a standardized drought indexing approach that allows us to directly compare, for any given location of

interest, its moisture status during different time windows, regardless of their length. For example, the FHM 2010 national report includes a comparison of national drought maps for 2009, the 3-year window of 2007–09, and the 5-year window of 2005–09 (Koch and others, 2013).

One of our main goals for the current analysis was to apply the methodology devised for the FHM 2010 national report to the most recently available climate data, i.e., the monthly PRISM data through 2010, thus providing a second time step in what we anticipate to be an ongoing annual record of drought status across the conterminous United States from 2009 forward. In addition, we performed a separate national-scale analysis in which we mapped, for the 100-year period from 1911 to 2010, the frequency of 2, 3, 4, and 5 consecutive years of moderate to extreme drought conditions during the late spring-early summer "season." We focused on this late spring-early summer period because it is a time of peak emergence for certain adult forest insect pests such as the emerald ash borer, *Agrilus planipennis* (Anulewicz and others 2008, Poland and McCullough 2006). Trees that experience acute drought stress during this period may be especially attractive hosts for the newly emerged adults and also more vulnerable to attack, promoting the likelihood of pest outbreaks (Guarín and Taylor 2005, Mattson and Haack 1987). Our interest in consecutive-year frequencies was driven by the idea that any geographic area where this late spring-early summer drought pattern tends to be repeated from year to year faces an even higher outbreak risk, and so should be prioritized for pest surveillance or other management activities.

METHODS

When we performed the analyses, monthly PRISM grids for total precipitation, mean daily minimum temperature, and mean daily maximum temperature were available from the PRISM group Web site (PRISM Group 2010) for all years from 1895 to 2010. Each gridded data set covered the entire conterminous United States. The spatial resolution of these input grids was approximately 4 km (cell area = 16 km^2). However, for the purpose of future applications and better compatibility with other spatial data sets, all output grids were resampled to a spatial resolution of approximately 2 km (cell area = 4 km^2) using a nearest neighbor approach.

Potential Evapotranspiration Maps

As in our previous work on drought (Koch and others 2012a, 2012b), we adopted an approach in which a moisture index value for each location of interest (i.e., each grid cell in a map of the conterminous United States) was calculated based on both precipitation and potential evapotranspiration values for that location during the time period of interest. Potential evapotranspiration measures the loss of soil moisture through plant uptake and transpiration (Akin 1991). It does not measure actual moisture loss, but rather the loss that would occur under ideal conditions, i.e., if there was no possible shortage of moisture for plants to transpire (Akin 1991, Thornthwaite 1948). The inclusion of both precipitation and

potential evapotranspiration provides a fuller accounting of a location's water balance than precipitation alone.

To complement the available PRISM monthly precipitation grids, we computed corresponding monthly potential evapotranspiration (*PET*) grids using the Thornthwaite formula (Akin 1991, Thornthwaite 1948):

$$PET_m = 1.6 L_{lm} (10 \frac{T_m}{I})^a \qquad (1)$$

where

PET_m = the potential evapotranspiration for a given month m in cm

L_{lm} = a correction factor for the mean possible duration of sunlight during month m for all locations, i.e., grid cells, at a particular latitude l [see table V in Thornthwaite (1948) for a list of L correction factors by month and latitude]

T_m = the mean temperature for month m in degrees C

I = an annual heat index, calculated as

$$I = \sum_{m=1}^{12} \left(\frac{T_m}{5} \right)^{1.514}$$

where

T_m = the mean temperature for each month m of the year

a = an exponent calculated as $a = 6.75 \times 10^{-7} I^3 - 7.71 \times 10^{-5} I^2 + 1.792 \times 10^{-2} I + 0.49239$ [see appendix I in Thornthwaite (1948) regarding the empirical derivation of a]

To implement equation 1 spatially, we created a grid of latitude values for determining the L adjustment for any given grid cell (and any given month) in the conterminous United States. We calculated the mean monthly temperature grids as the mean of the corresponding PRISM daily minimum and maximum monthly temperature grids.

Moisture Index Maps

We used the precipitation (*P*) and *PET* grids to generate baseline moisture index grids for the past 100 years (i.e., 1911–2010) for the conterminous United States. We used a moisture index, *MI'*, proposed by Willmott and Feddema (1992), which has the following form:

$$MI' = \begin{cases} P/PET - 1 & , \quad P < PET \\ 1 - PET/P & , \quad P \geq PET \\ 0 & , \quad P = PET = 0 \end{cases} \qquad (2)$$

where

P = precipitation

PET = potential evapotranspiration

(P and PET must be in equivalent measurement units, e.g., mm)

This set of equations yields a dimensionless index scaled between -1 and 1. *MI′* can be calculated for any time period, but is commonly calculated on an annual basis using summed *P* and *PET* values (Willmott and Feddema 1992). An alternative to this summation approach is to calculate *MI′* from monthly precipitation and potential evapotranspiration values and then, for a given time window of interest, calculate its moisture index as the mean of the *MI′* values for all months in the window. This "mean-of-months" approach limits the ability of short-term peaks in either precipitation or potential evapotranspiration to negate corresponding short-term deficits, as would happen under a summation approach.

For each year in our study period (1911–2010), we used the mean-of-months approach to calculate moisture index grids for three different time windows: 1 year (MI_1'), three years (MI_3'), and 5 years (MI_5'). Briefly, the MI_1' grids are the mean of the 12 monthly *MI′* grids for each year in the study period, the MI_3' grids are the mean of the 36 monthly grids from January 2 years prior through December of each year, and the MI_5' grids are the mean of the 60 consecutive monthly *MI′* grids from January 4 years prior to December of each year. For example, the MI_1' grid for the year 2010 is the mean of the monthly *MI′* grids from January to December 2010, while the MI_3' grid is the mean of grids from January 2008 to December 2010 and the MI_5' grid is the mean of the grids from January 2006 to December 2010.

Annual and Multi-Year Drought Maps

To determine degree of departure from typical moisture conditions, we first created a normal grid, $MI'_{i\ norm}$, for each of our three time windows, representing the mean of the 100 corresponding moisture index grids (i.e., the MI_1', MI_3', or MI_5' grids, depending on the window; see fig. 4.1). We also created a standard deviation grid, $MI'_{i\,SD}$, for each time window, calculated from the window's 100 individual moisture index grids as well as its $MI'_{i\ norm}$ grid. We subsequently calculated moisture difference *z*-scores, MDZ_j, for each time window using these gridded data sets:

$$MDZ_{ij} = \frac{MI_i' - MI_{i\ norm}'}{MI_{i\ SD}'} \qquad (3)$$

where

i = the analytical time window (1, 3, or 5 years)

j = a particular target year in our 100-year study period (i.e., 1911-2010)

MDZ scores may be classified in terms of degree of moisture deficit or surplus (table 4.1). The classification scheme includes categories, e.g., severe drought, extreme drought, like those associated with the Palmer Drought Severity Index (PDSI) (Palmer 1965). Importantly, because of the standardization in equation 3, the breakpoints between categories remain the same regardless of the size of the time window of interest. For comparative analysis, we generated classified *MDZ* maps, based on all three time

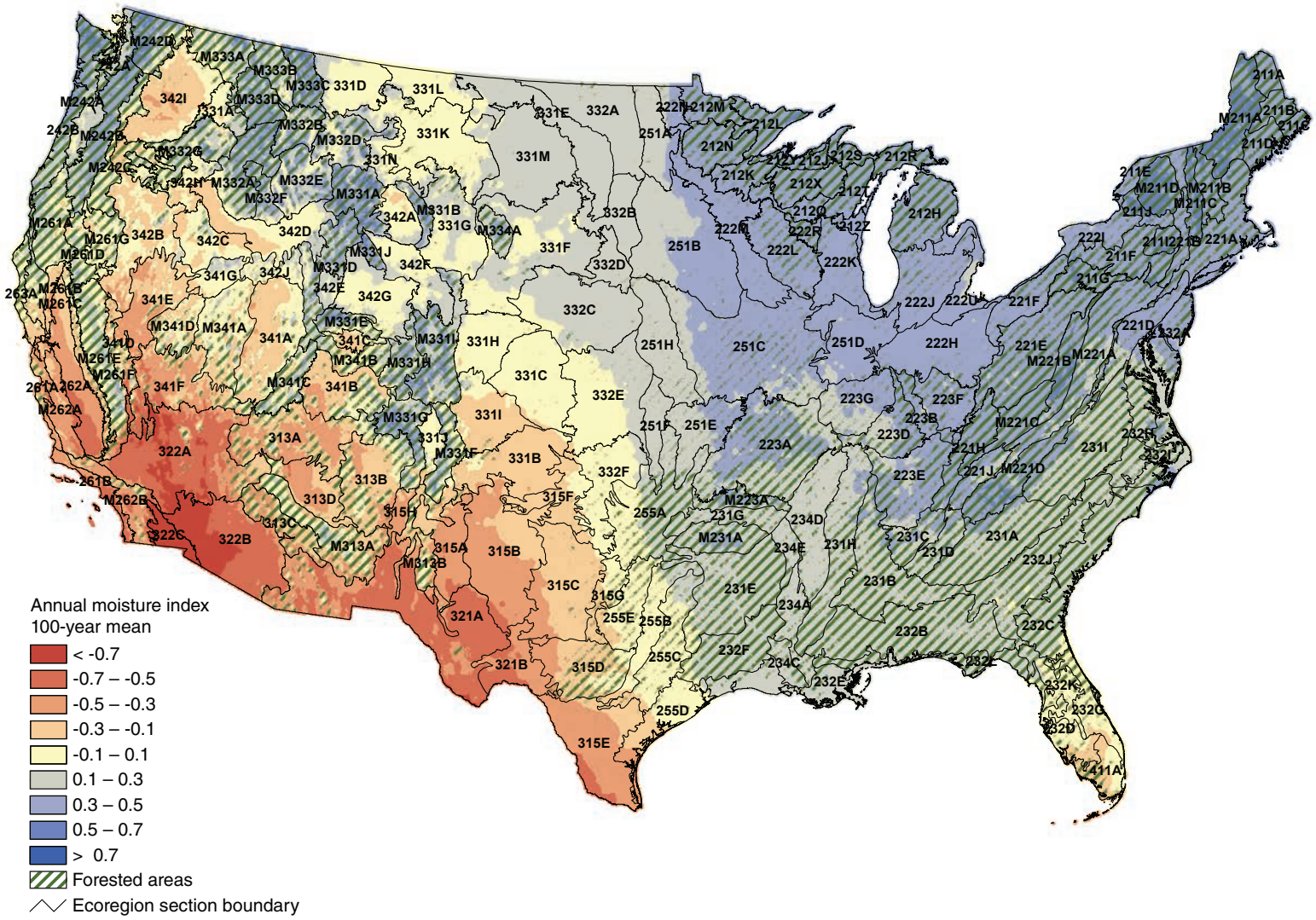

Figure 4.1—The 100-year (1911–2010) mean annual moisture index, or MI_1'*, for the conterminous United States. Ecoregion section (Cleland and others 2007) boundaries and labels are included for reference. Forest cover data (overlaid green hatching) derived from Moderate Resolution Imaging Spectroradiometer (MODIS) imagery by the USDA Forest Service, Remote Sensing Applications Center. (Data source: PRISM Group, Oregon State University.)*

windows, for the target year 2010 (figs. 4.2–4.4). Because our analysis focused on drought (i.e., moisture deficit) conditions, we combined the four moisture surplus categories from table 4.1 into a single category for map display.

Frequency of Consecutive Years of Late Spring-Early Summer Drought

As opposed to the mean-of-months approach used in the previously described analyses, for the late spring-early summer drought analysis we calculated *MI′* (equation 2) based on the total *P* and *PET* values summed over a 3-month period. Notably, late spring-early summer represents a different time window depending on geographic location within the conterminous United States, i.e., depending on latitude, elevation, and climatic regime. Hence, we actually calculated nationwide *MI′* grids for three different 3-month windows during each year of our 1911–2010 study period: March-May, April-June, and May-July. For each of these 3-month windows, we next calculated distinct MI'_{norm} and MI'_{SD} grids based on the window's 100 individual *MI′* grids calculated for each year of our study period. We then applied equation 3 to generate distinct *MDZ* grids for each window in each year. (In this context, the index *i* in equation 3 should be interpreted as corresponding to one of the 3-month windows rather than the 1-, 3-, or 5-year windows discussed previously.)

To combine the March-May, April-June, and May-July *MDZ* grids for each year into a single nationwide grid depicting late spring-early summer moisture conditions, we first subset them using spatial data related to frost-free period. These data served to represent the approximate beginning of spring and the growing season. Briefly, we divided the conterminous United States into three geographic regions (fig. 4.5) based on the 30-year mean Julian date of the last spring freeze: Zone 1, including all areas with a mean Julian date ≤ 90, i.e., last freeze prior to April 1; Zone 2, all areas with a mean Julian date between 90 and 120, i.e., last freeze between April 1 and April 30; and Zone 3, all areas with a mean Julian date > 120, i.e., last freeze after April 30. Next, we matched each 3-month window to the most appropriate zone (fig. 4.5), and then clipped the corresponding *MDZ* grid to the zonal boundaries. Finally, we created a mosaic of these clipped grids, combining them into a single late spring-early summer grid that covers the conterminous United States.

Table 4.1—Moisture difference z-score (*MDZ*) value ranges for nine wetness and drought categories, along with each category's approximate theoretical frequency of occurrence

MDZ Score	Category	Frequency
<-2	Extreme drought	2.3%
-2 to -1.5	Severe drought	4.4%
-1.5 to -1	Moderate drought	9.2%
-1 to -0.5	Mild drought	15%
-0.5 to 0.5	Near normal conditions	38.2%
0.5 to 1	Mild moisture surplus	15%
1 to 1.5	Moderate moisture surplus	9.2%
1.5 to 2	Severe moisture surplus	4.4%
> 2	Extreme moisture surplus	2.3%

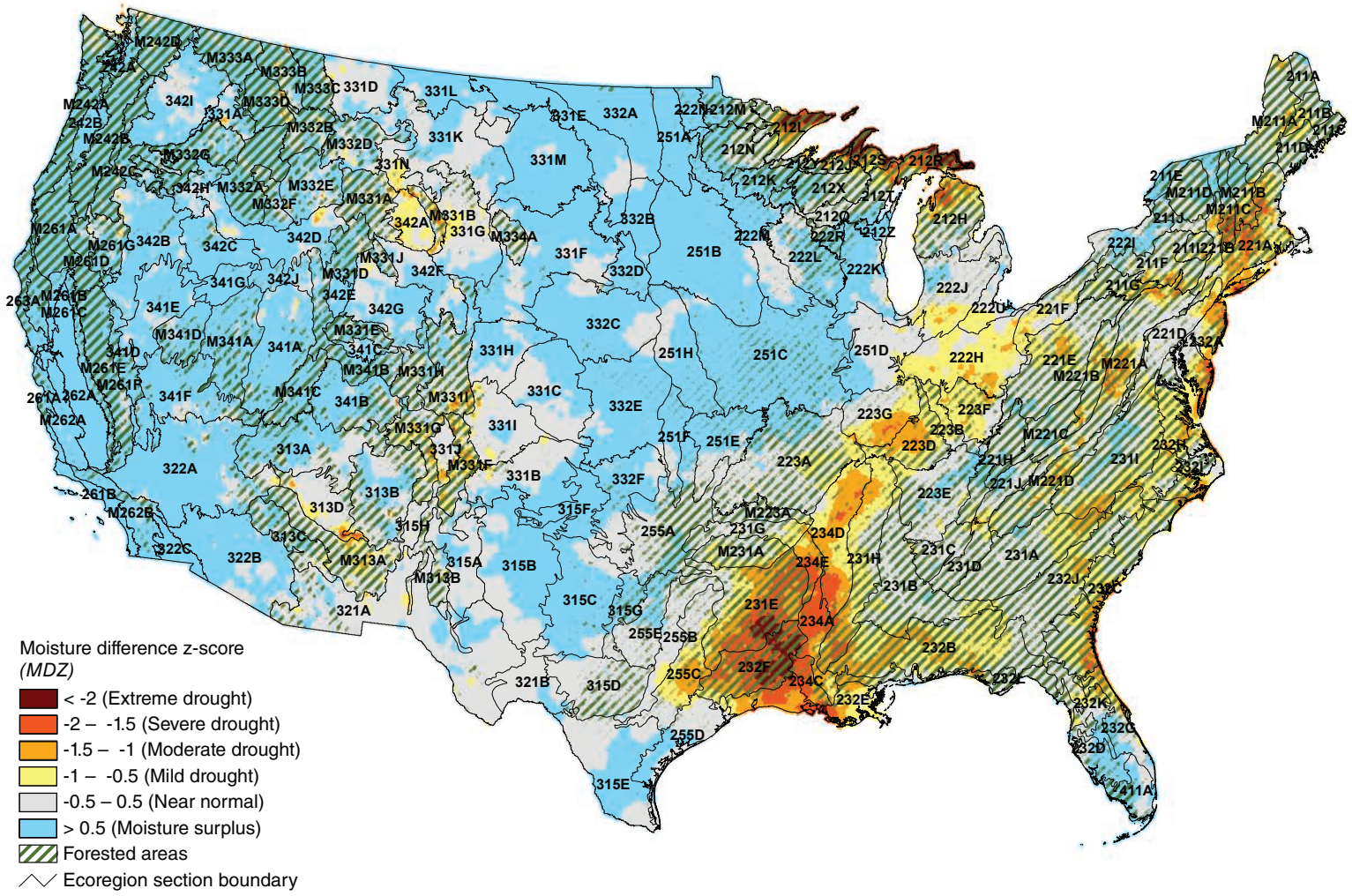

Figure 4.2—The 2010 annual (i.e., 1-year) moisture difference z-score, or MDZ, *for the conterminous United States. Ecoregion section (Cleland and others 2007) boundaries and labels are included for reference. Forest cover data (overlaid green hatching) derived from MODIS imagery by the USDA Forest Service, Remote Sensing Applications Center. (Data source: PRISM Group, Oregon State University.)*

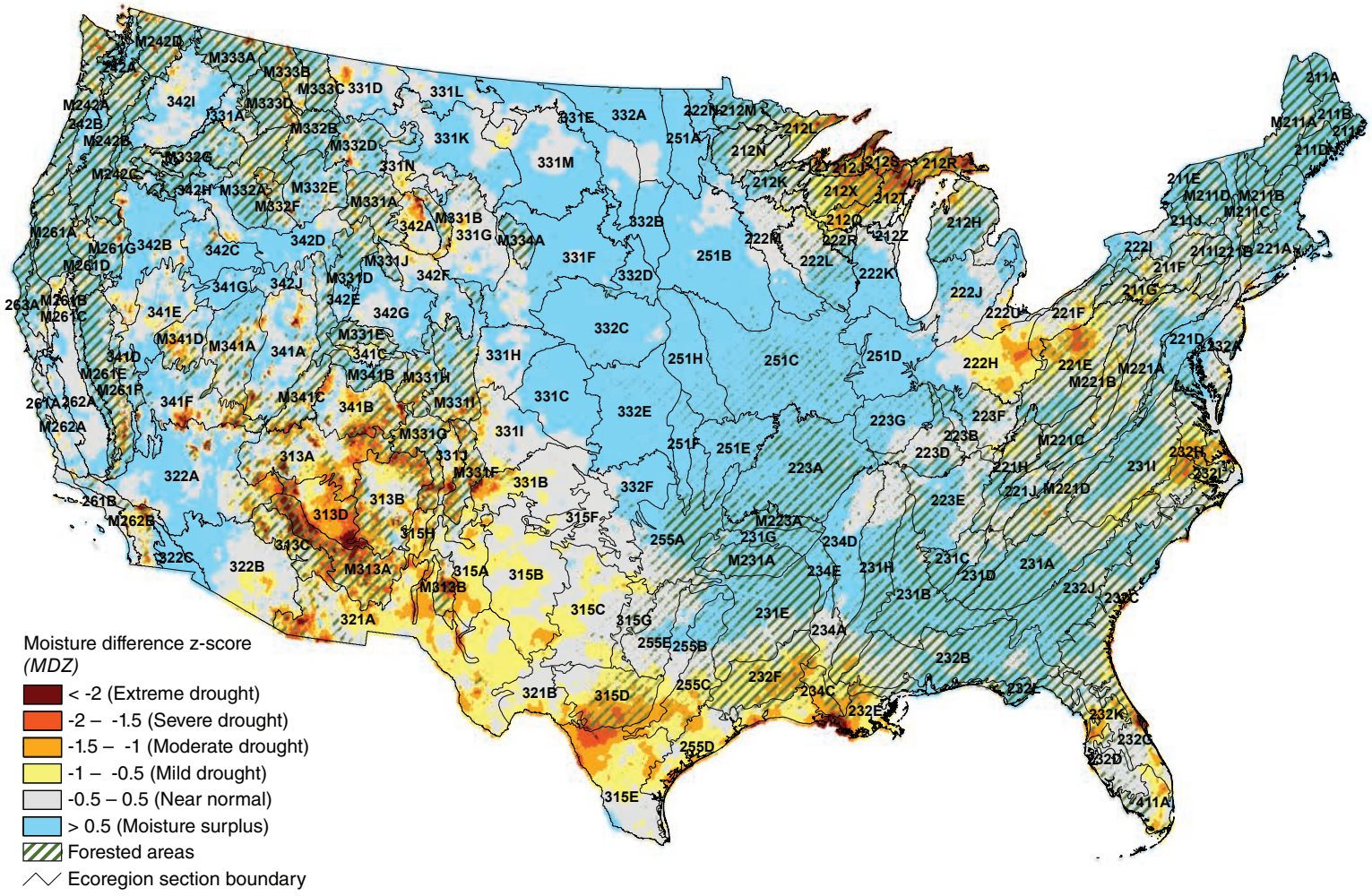

Figure 4.3—The 2008–10 (i.e., 3-year) moisture difference z-score, or MDZ, *for the conterminous United States. Ecoregion section (Cleland and others 2007) boundaries are included for reference. Forest cover data (overlaid green hatching) derived from MODIS imagery by the USDA Forest Service, Remote Sensing Applications Center. (Data source: PRISM Group, Oregon State University.)*

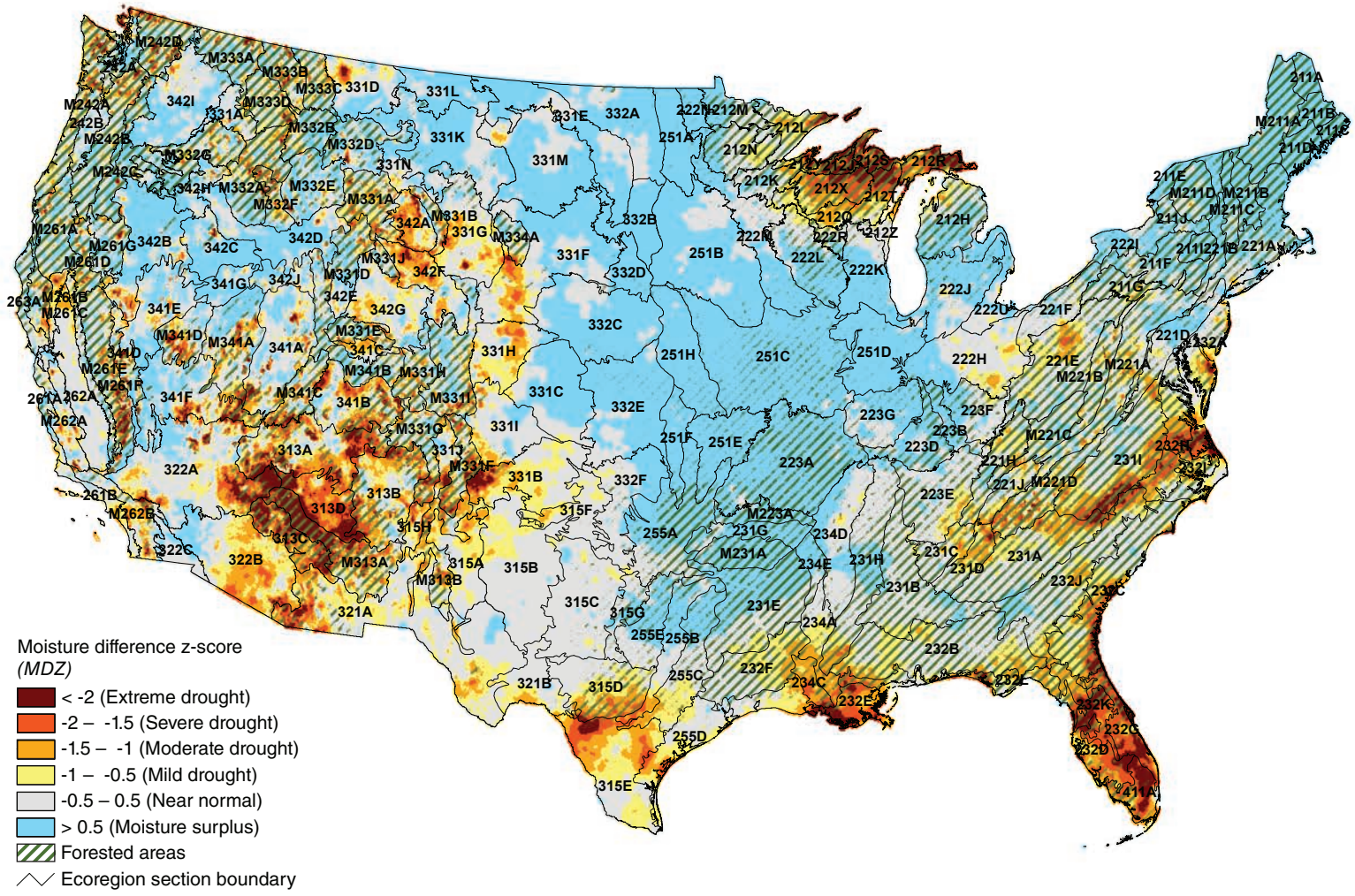

Figure 4.4—The 2006–10 (i.e., 5-year) moisture difference z-score, or MDZ, *for the conterminous United States. Ecoregion section (Cleland and others 2007) boundaries are included for reference. Forest cover data (overlaid green hatching) derived from MODIS imagery by the USDA Forest Service, Remote Sensing Applications Center. (Data source: PRISM Group, Oregon State University.)*

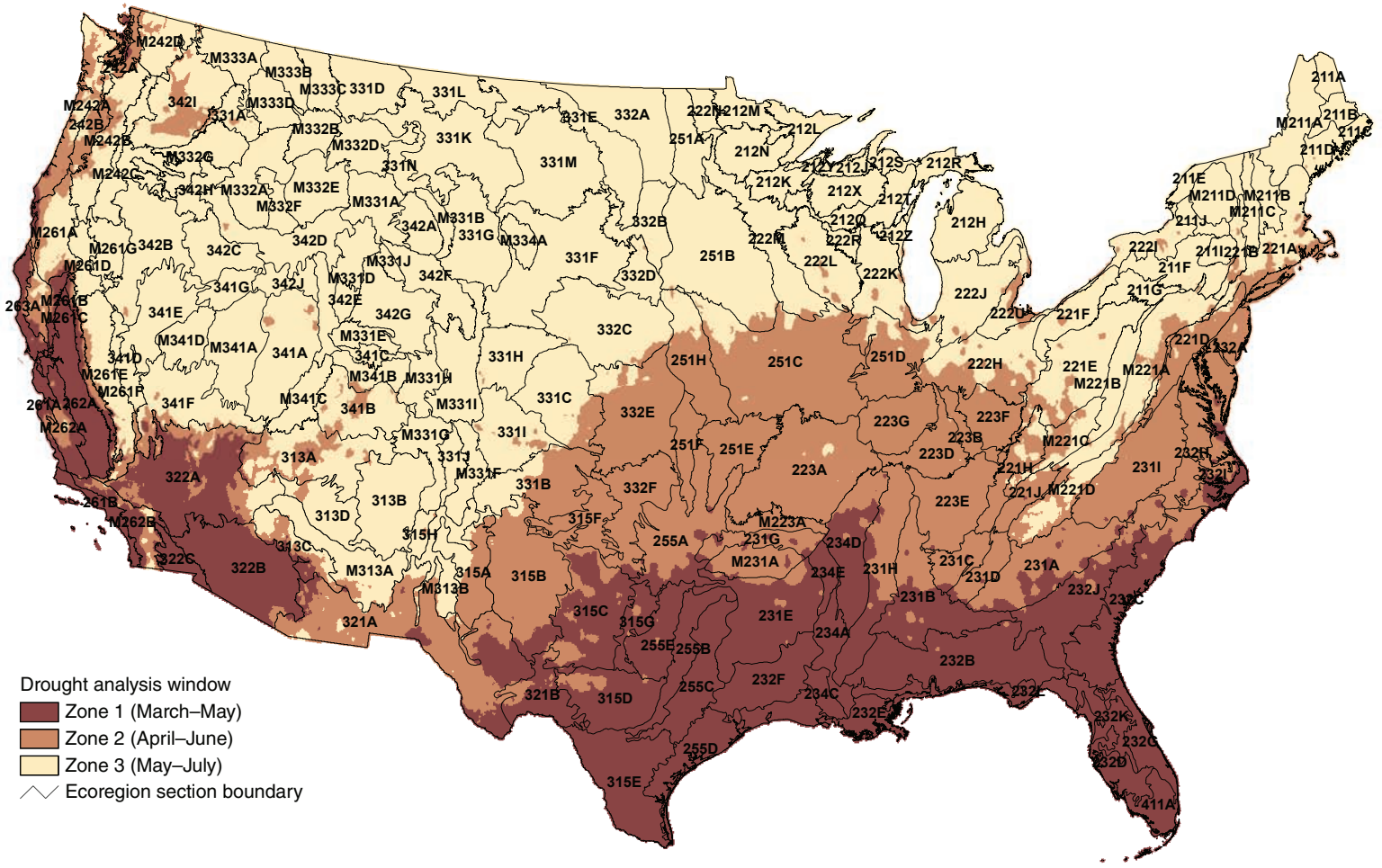

Figure 4.5—Three analysis zones, each corresponding to a particular 3-month time window used when calculating late spring-early summer drought conditions for the associated areas of the conterminous United States. Ecoregion section (Cleland and others 2007) boundaries and labels are included for reference. Zones were developed from data describing frost-free period. (Data source: The Climate Source, LLC, Corvallis, OR.)

To estimate consecutive-year drought frequencies, we began by generating a binary grid from each late spring-early summer grid, assigning all grid cells with *MDZ* values less than -1, i.e., exhibiting moderate to extreme drought stress, a value of 1 and all other cells a value of 0. We stacked the 100 resulting binary grids in annual order, from 1911 to 2010, creating a geographically referenced, three-dimensional array; conceptually, each geographic location, i.e., each grid cell in a map of the conterminous United States, was represented by a vector, *V*, containing 100 temporally ordered elements (indexed by $x = 1\ldots100$) with a value of 0 or 1. We analyzed each vector *V* element-by-element to tally the following frequencies (fig. 4.6): (1) the number of times that V_x and V_{x-1} were both equal to 1, indicating 2 consecutive years of moderate to extreme drought during the late spring-early summer season; (2) the number of times that V_x, V_{x-1}, and V_{x-2} were all equal to 1, indicating 3 consecutive years of moderate to extreme drought; (3) the number of times that V_x, V_{x-1}, V_{x-2}, and V_{x-3} were all equal to 1, indicating 4 consecutive years of moderate to extreme drought; and (4) the number of times that V_x, V_{x-1}, V_{x-2}, V_{x-3}, V_{x-4} were all equal to 1, indicating 5 consecutive years of moderate to extreme drought during the late spring-early summer.

RESULTS AND DISCUSSION

The 100-year (1911–2010) mean annual moisture index, or MI_1', grid (fig. 4.1) provides a general illustration of climatic regimes across the conterminous United States. (Because the 100-year mean MI_3' and MI_5' grids were only negligibly different from the mean MI_1' grid, they are not shown here.) In general, wet climates ($MI' > 0$) are characteristic through the Eastern United States, especially the Northeast. Notably, it appears that southern Florida (in particular, ecoregion sections 232C-Florida Coastal Lowlands-Atlantic, 232D-Florida Coastal Lowlands-Gulf, and 411A-Everglades) is the driest region of the Eastern United States. Although this region typically has a high level of precipitation, this is more than offset by a high level of potential evapotranspiration, resulting in negative *MI′* values. This explanation for the relative dryness of southern Florida, i.e., high *P* offset by high *PET*, differs from the circumstances in the driest regions of the Western United States, particularly the Southwest, e.g., sections 322A-Mojave Desert, 322B-Sonoran Desert, and 322C-Colorado Desert, where potential evapotranspiration is very high but precipitation levels are usually very low. In fact, dry climates ($MI' < 0$) are common across much of the Western United States because of generally lower precipitation than the East. However, mountainous areas in the central and northern Rocky Mountains as well as the Pacific Northwest are relatively wet, e.g., ecoregion sections M242A-Oregon and Washington Coast Ranges, M242B-Western Cascades, M331G-South-Central Highlands, and M333C-Northern Rockies. This is at least partially shaped by high levels of winter snowfall.

Figure 4.2 shows the annual (1-year) *MDZ* map for 2010 for the conterminous United

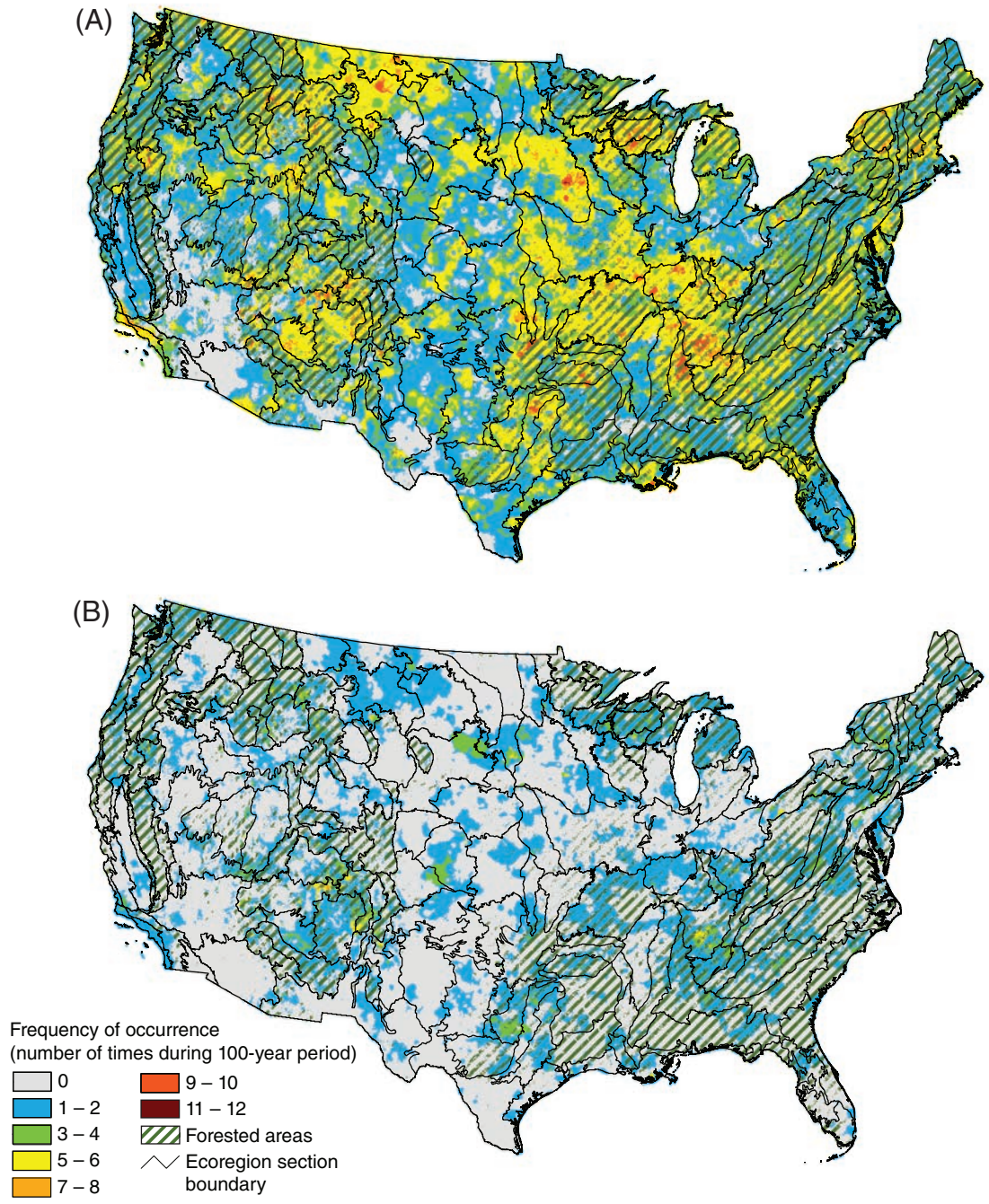

Figure 4.6—Over a 100-year period (1911–2010), the frequency of: (A) 2 consecutive years of moderate to extreme drought conditions during the late spring-early summer for the conterminous United States; (B) 3 consecutive years of moderate to extreme drought during late spring-early summer; (C) 4 consecutive years of moderate to extreme drought during late spring-early summer; and (D) 5 consecutive years of moderate to extreme drought during late spring-early summer. Ecoregion section (Cleland and others 2007) boundaries are included for reference. (Data source: PRISM Group, Oregon State University.) *(continued on next page)*

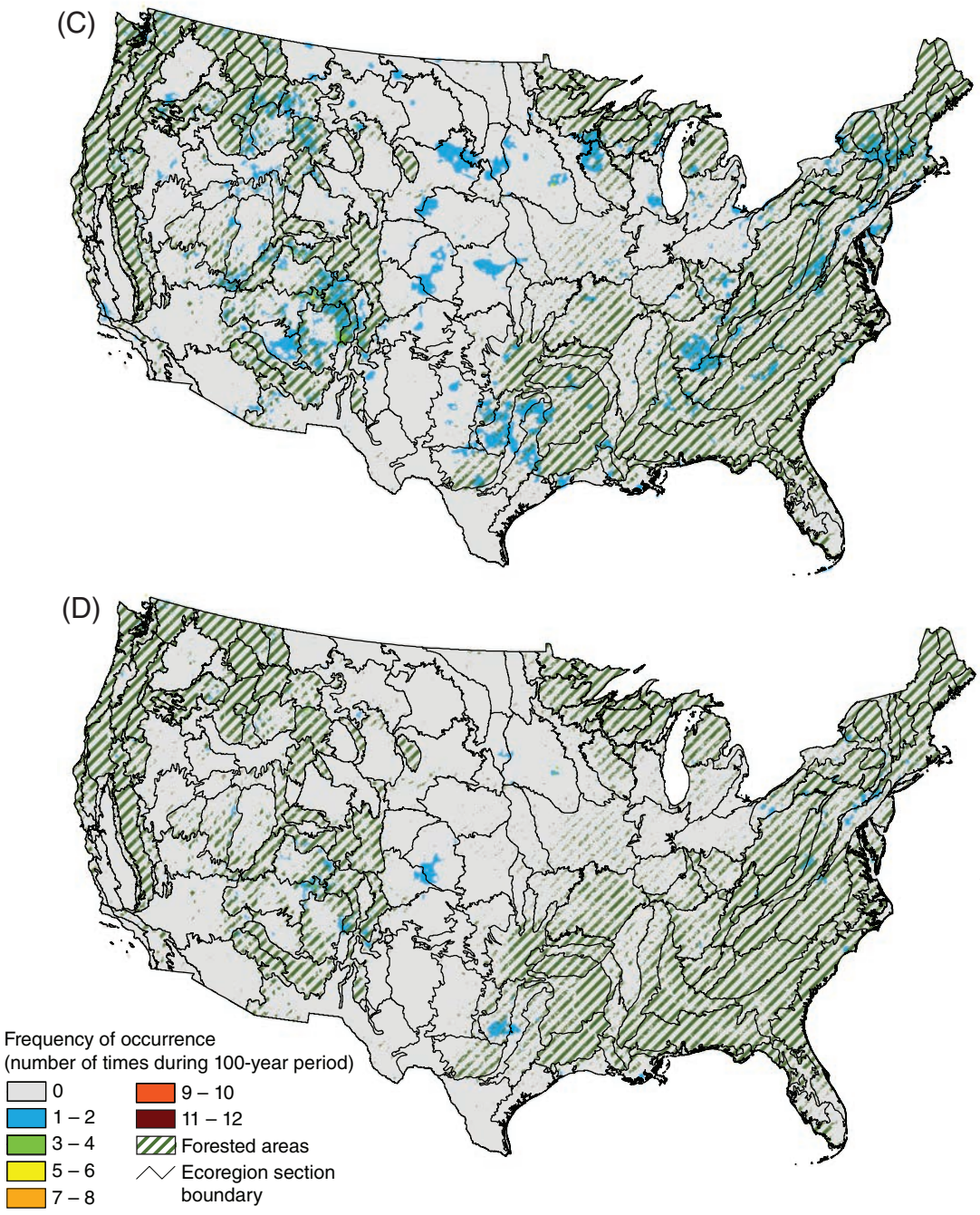

Figure 4.6 (continued)—Over a 100-year period (1911–2010), the frequency of: (A) 2 consecutive years of moderate to extreme drought conditions during the late spring-early summer for the conterminous United States; (B) 3 consecutive years of moderate to extreme drought during late spring-early summer; (C) 4 consecutive years of moderate to extreme drought during late spring-early summer; and (D) 5 consecutive years of moderate to extreme drought during late spring-early summer. Ecoregion section (Cleland and others 2007) boundaries are included for reference. (Data source: PRISM Group, Oregon State University.)

States. Most of the Western United States experienced a moisture surplus in 2010, although there were scattered pockets of moderate to extreme drought, largely limited to ecoregion sections (Cleland and others 2007) in the Rocky Mountain region such as M331B-Bighorn Mountains, M331F-Southern Parks and Rocky Mountain Range, M331G-South Central Highlands, and M331I-Northern Parks and Ranges (as well as the southeastern tip of 313D-Painted Desert, an area that is largely non-forested). This pattern of general moisture surplus in the West is a significant departure from a trend of intense and prolonged region-wide drought during most of the last decade (Groisman and Knight 2008, Mueller and others 2005, NOAA 2010, 2011, O'Driscoll 2007). In contrast, there were fairly extensive areas of drought in the Eastern United States during 2010. Two areas are particularly noteworthy. The first is a large "hot spot" of drought in the Southeastern United States along the central coast of the Gulf of Mexico. This hot spot is centered on the heavily forested sections 231E-Mid Coastal Plains-Western and 232F-Coastal Plains and Flatwoods-Western Gulf, each of which had large areas of severe to extreme drought during 2010. The adjacent (and less heavily forested) sections 232E-Louisiana Coastal Prairie and Marshes, 234A-Southern Mississippi Alluvial Plain, 234C-Atchafalaya and Red River Alluvial Plains, and 234E-Arkansas River Alluvial Plain also contained sizeable areas of severe drought. By way of an explanation, this geographic region had near-record dry conditions throughout the spring and summer of 2010, which was further amplified by record high summer temperatures (NOAA 2011). These conditions have been linked to a marked increase in *Ips* bark beetle damage in this region, resulting in scattered mortality of thousands of trees and, occasionally, high mortality in individual forest stands (Louisiana Department of Agriculture and Forestry 2011). The second hot spot of note is the western Great Lakes region, particularly the heavily forested sections 212L-Northern Superior Uplands, 212R-Eastern Upper Peninsula, and 212S-Northern Upper Peninsula, all of which contained large areas of severe to extreme drought. This portion of the Great Lakes region experienced record dryness during the spring of 2010 (NOAA 2011).

Besides these two prominent drought hot spots, there were numerous pockets of drought distributed across the Eastern United States in 2010 (fig. 4.2). Foremost is a distinctive pattern of moderate to extreme drought along much of the Atlantic Coast, especially in the forested ecoregion sections 221A-Lower New England, 232A-Northern Atlantic Coastal Plain, 232C-Atlantic Coastal Flatwoods, 232H-Middle Atlantic Coastal Plains and Flatwoods, and 232I-Northern Atlantic Coastal Flatwoods. This pattern appears to have been influenced by hot, dry weather that occurred in the region from July to September 2010 (NOAA 2011, NDMC 2011).

When combined with the annual (i.e., single-year) *MDZ* map in figure 4.2, the 3-year (fig. 4.3) and 5-year (fig. 4.4) *MDZ* maps provide an overview of the recent chronology of moisture

conditions in the conterminous United States. For instance, the persistent drought conditions that affected much of the Western United States, and especially the Desert Southwest region, during the last decade (Groisman and Knight 2008; Mueller and others 2005; NOAA 2010, 2011; O'Driscoll 2007) are partially captured by the 3-year and 5-year *MDZ* maps. (These two maps contrast strongly with the annual *MDZ* map, which supports the notion that the observed pattern of moisture surplus throughout most of the West in 2010 represents a substantial departure from the region's recent history.)

Additionally, the drought hot spot that appeared in the Great Lakes region during 2010 (see fig. 4.2) is also reflected in the 3-year and 5-year *MDZ* maps, suggesting that drought stress may be a persistent problem for forests in this region. This may similarly be true regarding the previously described hot spot on the central Gulf Coast. It is worth mentioning that in these geographic regions as well as others (e.g., central to southern Florida) the 5-year *MDZ* map (fig. 4.4) appears to show more extensive and/or severe drought conditions than the 3-year *MDZ* map (fig. 4.3). This discrepancy between maps may indicate temporally variable, yet fundamentally persistent, drought conditions in a region of interest, as is the case for the Western United States. However, it may instead be explained by the occurrence of markedly bad drought conditions at some point during the first 2 years of the 5-year *MDZ* window, i.e., 2006–07 for the current analysis. For example, a portion of the Southeastern United States, i.e., parts of sections 231I-Central Appalachian Piedmont, 232H-Middle Atlantic Coastal Plain and Flatwoods, and 232I-Northern Atlantic Coastal Plain and Flatwoods, showed substantially worse drought conditions in the 5-year *MDZ* map than in the 3-year map; a historically exceptional drought that occurred during 2007 (O'Driscoll 2007) is probably the major factor behind this difference. Thus, while the 1-year, 3-year, and 5-year *MDZ* maps together provide a fairly comprehensive short-term overview, it may be additionally important to consider a particular region's longer-term drought history when evaluating the current health level of the region's forests.

With respect to the late spring-early summer drought frequency maps (fig. 4.6), no especially strong geographic pattern emerges, although some parts of the conterminous United States may benefit from further investigation. For example, figure 4.6A highlights a number of areas where two consecutive years of moderate or worse late spring-early summer drought occurred nine or more times between 1911 and 2010; because this represents a fairly large proportion of our 100-year study period, it seems reasonable to assume these highlighted areas face an elevated risk of outbreaks of certain forest pests. Two geographic regions contain the largest clusters of high-frequency areas and may therefore deserve additional attention: the south-central United States (particularly the forested ecoregion sections 223E-Interior Low Plateau-Highland Rim and 231B-Coastal Plains-Middle) and the western

Great Lakes region (particularly the forested sections 212Q-North Central Wisconsin Uplands and 212X-Northern Highlands).

Despite lacking a strong pattern, the moderate level of spatial variability in the 2-consecutive-year drought map suggests that it might serve well as an input to future pest risk mapping projects, i.e., as an additional discriminatory layer to complement data on host distribution, pathways of introduction, and the pest's environmental constraints. In contrast, perhaps the most important thing demonstrated by the 3-, 4- and 5-consecutive-year drought maps (figs. 4.6B–4.6D) is that very little of the country is likely to see a protracted pattern of repeated late spring-early summer droughts. A few ecoregion sections did have small areas where there were multiple, i.e., five or more, occurrences of 3 consecutive years of late spring-early summer drought during our study period (fig. 4.6B), such as the aforementioned section 223E in the south-central United States, and in the West, sections 313A-Grand Canyon and M331G-South Central Highlands. However, < 8 percent of the conterminous United States saw 4 consecutive years of late spring-early summer occur at least once during our 100-year study period, and only 0.2 percent saw this happen more than twice. Furthermore, just over 1 percent of the country experienced 5 consecutive years of late spring-early summer drought at any point during the study period.

A similar set of consecutive-year frequency maps could be produced for any season deemed relevant to a particular forest health issue, e.g., to test drought-related hypotheses pertaining to the issue. In addition to this type of on-demand product, and assuming the spatial data, i.e., the high-resolution maps of precipitation and temperature, underlying these analyses continue to be available for public use, we expect to produce our 1-year, 3-year, and 5-year *MDZ* maps in the future as a standard component of national-scale forest health reporting. Nevertheless, it is important for users to interpret and compare the *MDZ* drought maps cautiously. Although the maps use a standardized index scale that applies regardless of the size of the time window, it should also be understood that, for instance, an extreme drought, i.e., where *MDZ* < -2, that persists over a 5-year period has substantially different forest health implications than an extreme drought over a 1-year period. In future work, we hope to provide forest managers and other decisionmakers with better quantitative evidence regarding some of these relationships between drought and forest health.

LITERATURE CITED

Akin, W.E. 1991. Global patterns: climate, vegetation, and soils. Norman, OK: University of Oklahoma Press. 370 p.

Anulewicz, A.C.; McCullough, D.G.; Cappaert, D.L.; Poland, T.M. 2008. Host range of the emerald ash borer (*Agrilus planipennis* Fairmaire) (Coleoptera: Buprestidae) in North America: results of multiple-choice field experiments. Environmental Entomology. 37(1): 230-241.

Archaux, F.; Wolters, V. 2006. Impact of summer drought on forest biodiversity: what do we know? Annals of Forest Science. 63: 645-652.

Clark, J.S. 1989. Effects of long-term water balances on fire regime, north-western Minnesota. Journal of Ecology. 77: 989-1004.

Cleland, D.T.; Freeouf, J.A.; Keys, J.E., Jr. [and others]. 2007. Ecological subregions: sections and subsections for the conterminous United States. Sloan, A.M., tech. ed. Gen. Tech. Rep. WO-76. Washington, DC: U.S. Department of Agriculture Forest Service. Map, presentation scale 1:3,500,000; Albers equal area projection; colored. Also as a GIS coverage in ArcINFO format on CD-ROM or at http://fsgeodata.fs.fed.us/other_resources/ecosubregions.html. [Date accessed: May 9, 2011].

Clinton, B.D.; Boring, L.R.; Swank, W.T. 1993. Canopy gap characteristics and drought influences in oak forests of the Coweeta Basin. Ecology. 74(5): 1551-1558.

Daly, C.; Gibson, W.P.; Taylor, G.H. [and others]. 2002. A knowledge-based approach to the statistical mapping of climate. Climate Research. 22: 99-113.

Groisman, P.Y.; Knight, R.W. 2008. Prolonged dry episodes over the conterminous United States: new tendencies emerging during the last 40 years. Journal of Climate. 21: 1850-1862.

Guarín, A.; Taylor, A.H. 2005. Drought triggered tree mortality in mixed conifer forests in Yosemite National Park, California, USA. Forest Ecology and Management. 218: 229-244.

Hanson, P.J.; Weltzin, J.F. 2000. Drought disturbance from climate change: response of United States forests. The Science of the Total Environment. 262: 205-220.

Hinckley, T.M.; Dougherty, P.M.; Lassoie, J.P. [and others]. 1979. A severe drought: impact on tree growth, phenology, net photosynthetic rate, and water relations. American Midland Naturalist. 102(2): 307-316.

Kareiva, P.M.; Kingsolver, J.G.; Huey, B.B., eds. 1993. Biotic interactions and global change. Sunderland, MA: Sinauer Associates, Inc. 559 p.

Keetch, J.J.; Byram, G.M. 1968. A drought index for forest fire control. Res. Pap. SE-38. Asheville, NC: U.S. Department of Agriculture Forest Service, Southeastern Forest Experiment Station. 33 p.

Koch, F.H.; Coulston, J.W.; Smith, W.D. 2012a. High-resolution mapping of drought conditions. In: Potter, K.M.; Conkling, B.L., eds. Forest health monitoring: 2008 national technical report. Gen. Tech, Rep. SRS-158. Asheville, NC: U.S. Department of Agriculture Forest Service, Southern Research Station: 45-62. Chapter 4.

Koch, F.H.; Coulston, J.W.; Smith, W.D. 2012b. Mapping drought conditions using multi-year windows. In: Potter, K.M.; Conkling, B.L., eds. Forest health monitoring: 2009 national technical report. Gen. Tech. Rep. SRS-167. Asheville, NC: U.S. Department of Agriculture Forest Service, Southern Research Station: 163-179. Chapter 10.

Koch, F.H.; Smith, W.D.; Coulston, J.W. 2013. An improved method for standardized mapping of drought conditions. In: Potter, K.M.; Conkling, B.L., eds. Forest health monitoring: national status, trends, and analysis 2010. Gen. Tech. Rep. SRS-176. Asheville, NC: U.S. Department of Agriculture Forest Service, Southern Research Station: 67-83. Chapter 6.

Louisiana Department of Agriculture and Forestry. 2011. Louisiana forest health highlights 2010. http://fhm.fs.fed.us/fhh/fhh_10/la_fhh_10.pdf. [Date accessed: November 9, 2011].

Mattson, W.J.; Haack, R.A. 1987. The role of drought in outbreaks of plant-eating insects. BioScience. 37(2): 110-118.

McDowell, N.; Pockman, W.T.; Allen, C.D. [and others]. 2008. Mechanisms of plant survival and mortality during drought: why do some plants survive while others succumb to drought? New Phytologist. 178: 719-739.

Millar, C.I.; Westfall, R.D.; Delany, D.L. 2007. Response of high-elevation limber pine (*Pinus flexilis*) to multiyear droughts and 20th-century warming, Sierra Nevada, California, USA. Canadian Journal of Forest Research. 37: 2508-2520.

Mueller, R.C.; Scudder, C.M.; Porter, M.E. [and others]. 2005. Differential tree mortality in response to severe drought: evidence for long-term vegetation shifts. Journal of Ecology. 93: 1085-1093.

National Climatic Data Center. 2007. Time bias corrected divisional temperature-precipitation-drought index. Documentation for dataset TD-9640. http://www1.ncdc.noaa.gov/pub/data/cirs/drought.README. [Date accessed: July 20, 2010].

National Climatic Data Center. 2010. State of the climate - drought - annual report 2009 [web page]. http://www.ncdc.noaa.gov/sotc/2009/13. [Date accessed: May 12, 2011].

National Climatic Data Center. 2011. State of the climate - drought - annual report 2010 [web page]. http://www.ncdc.noaa.gov/sotc/drought/2010/13. [Date accessed: May 10, 2011].

National Drought Mitigation Center). 2011. U.S. drought monitor GIS data archive. http://drought.unl.edu/dm/dmshps_archive.htm. [Date accessed: May 12, 2011].

National Oceanic and Atmospheric Administration. 2007. Time bias corrected divisional temperature-precipitation-drought index. Documentation for dataset TD-9640. http://www1.ncdc.noaa.gov/pub/data/cirs/drought.README. [Date accessed: July 20, 2010].

National Oceanic and Atmospheric Administration. State of the Climate: Drought Annual Report 2009. http://www.ncdc.noaa.gov/sotc/2009/13. [Date accessed: May 12, 2011].

National Oceanic and Atmospheric Administration. State of the Climate: Drought Annual Report 2010 [web page]. http://www.ncdc.noaa.gov/sotc/drought/2010/13. [Date accessed: May 10, 2011].

O'Driscoll, P. 2007. A drought for the ages; from the dried lake beds of Florida to the struggling ranches of California, a historic lack of rain is changing how Americans live. USA Today. June 8: 1A.

Palmer, W.C. 1965. Metereological drought. Res. Pap. No. 45. Washington, DC: U.S. Department of Commerce, Weather Bureau. 58 p.

Poland, T.M.; McCullough, D.G. 2006. Emerald ash borer: invasion of the urban forest and the threat to North America's ash resource. Journal of Forestry. 104(3): 118-124.

PRISM Group. 2010. 2.5-arcmin (4 km) gridded monthly climate data. ftp://prism.oregonstate.edu//pub/prism/us/grids. [Date accessed: September 16, 2010].

Schoennagel, T.; Veblen, T.T.; Romme, W.H. 2004. The interaction of fire, fuels, and climate across Rocky Mountain forests. BioScience. 54(7): 661-676.

Svoboda, M.; LeComte, D.; Hayes, M. [and others]. 2002. The drought monitor. Bulletin of the American Meteorological Society. 83(8): 1181-1190.

Thornthwaite, C.W. 1948. An approach towards a rational classification of climate. Geographical Review. 38(1): 55-94.

Willmott, C.J.; Feddema, J.J. 1992. A more rational climatic moisture index. Professional Geographer. 44(1): 84-87.